Article

First Live-Experience Session with PET/CT Specimen Imager. A pilot analysis in Prostate Cancer and Neuroendocrine Tumor.

Lorenzo Muraglia[1], Francesco Mattana[1], Laura Lavinia Travaini[1], Gennaro Musi[2,3], Emilio Bertani[4], Giuseppe Renne[5], Eleonora Pisa[5], Mahila Esmeralda Ferrari[6], Uberto Fumagalli Romario[4], Ottavio De Cobelli[2,3], Nicola Fusco[3,5] and Francesco Ceci[1,3]

[1] Division of Nuclear Medicine, IEO European Institute of Oncology IRCCS, Milan, Italy
[2] Division of Urology, IEO European Institute of Oncology IRCCS, Milan, Italy
[3] Department of Oncology and Hemato-Oncology, University of Milan, Milan, Italy
[4] Division of Digestive Surgery, IEO European Institute of Oncology IRCCS, Milan, Italy
[5] Division of Pathology, IEO European Institute of Oncology IRCCS, Milan, Italy
[6] Unit of Medical Physics, IEO European Institute of Oncology IRCCS, Milan, Italy
* Correspondence: **Author:** Francesco Ceci, MD PhD, Division of Nuclear Medicine IEO European Institute of Oncology IRCCS, Department of Oncology and Hemato-Oncology, University of Milan, Via Giuseppe Ripamonti, 43520141 Milan, Italy, E. francesco.ceci@ieo.it

Abstract: Objective: to evaluate the feasibility of the intra-operative application of a specimen PET/CT imager in a clinical setting. **Materials and methods:** this is a pilot analysis performed in three patients who received an intra-operative administration of ^{68}Ga-PSMA-11 (n=2) and ^{68}Ga-DOTA-TOC (n=1), respectively. Patients were administrated with PET radiopharmaceuticals to perform radio-guided surgery with a beta-probe detector during radical prostatectomy for prostate cancer (PCa) and salvage lymphadenectomy for recurrent neuroendocrine tumor (NET) of the ileum, respectively. All procedures have been performed within two ongoing clinical trials in our Institute (NCT05596851 and NCT05448157). Pathologic assessment with immunohistochemistry (PSMA-staining and SSA immunoreactivity) was considered as standard of truth. Specimen images were compared with baseline PET/CT images and histopathological analysis. **Results:** Patients received 1 MBq/Kg of ^{68}Ga-PSMA-11 (PCa) or 1.2 MBq/Kg of ^{68}Ga-DOTA-TOC (NET) prior to surgery. Specimens were collected, positioned in the dedicated specimen container, and scanned to obtain high resolution PET/CT images. In all cases a perfect match was observed between the findings detected by the specimen imager and histopathology. Overall, the PET spatial resolution was sensibly higher for the specimen images compared to the baseline whole-body PET/CT images. Furthermore, the use of the PET/CT specimen imager did not significantly interfere with any procedures, and the overall length of the surgery was not affected using the PET/CT specimen imager. Finally, the radiation exposure of the operating theater staff was lower than 40 μSv per procedure (range 26 – 40 μSv). **Conclusion:** the image acquisition of specimens obtained by patients who received intra-surgery injection of ^{68}Ga-PSMA-11 and ^{68}Ga-DOTA-TOC was feasible and reliable also in a live-experience session and has been easily adapted to surgery daily-practice. The high sensitivity, together with the evaluation of intra-lesion tumor heterogeneity, were the most relevant results since the data derived from specimen PET/CT imaging matched perfectly with the histopathological analysis.

Keywords: PET/CT; PET; PET/CT specimen imager; radio-guided surgery

1. Introduction

Positron Emission Tomography (PET) imaging is considered one of the leading imaging techniques to investigate oncological patients and it is considered the standard-of-care in many solid tumors and hematological malignancies (1). Recently, several technological improvements appeared in the field of PET imaging, ranging from digital detectors

 doi:10.20944/preprints202212.0444.v1

(e.g. silicon photomultipliers) to long axial field-of-view scanners (2). However, the attention moved also to smaller PET/computed tomography (CT) tomographs that might be implemented in the daily clinical practice of surgical oncology. Recently, a PET/CT specimen imager was developed to obtain full 3D high resolution images, assisting surgeons and pathologists during the surgical procedure directly in the operating theater. This specimen imager combines the picomolar sensitivity of PET (at sub-millimeter resolution) with anatomical information obtained from a high-resolution micro-CT. The first research application was in breast cancer using ^{18}F-FDG as a PET radiopharmaceutical, where a multicenter clinical trial is currently on-going (NCT04999917). Intra-operative high-resolution PET/CT imaging has shown promising results for margin assessment in breast malignancies, where a respective sensitivity and specificity of 84% and 96% was reached for the identification of positive margins of the invasive component of invasive ductal carcinoma (3). Explorative studies in pancreatic adenocarcinoma and in head and neck cancers have also demonstrated the feasibility of intra-operatively imaging radiotracer uptake in high resolution specimen PET/CT images (4,5).

Recently, novel radiopharmaceuticals emerged as game changers in prostate cancer (PCa) with prostate specific membrane antigen (PSMA) PET and in neuroendocrine tumor (NET) with somatostatin receptor (SSR) based PET. PSMA-PET showed its superiority compared to conventional imaging or other PET tracers in randomized clinical trials (6,7) or registry trials (8-10) to stage Pca or in case of disease recurrence, while SSR-agonist PET, is currently the standard-of-care to investigate gastro-entero-pancreatic NET (GEP-NET), especially in case of low-grade disease (G1-G2) (11). Furthermore, both PSMA inhibitors and SSR agonists are theranostic agents and can be labeled with isotopes for PET imaging (e.g. Gallium-68) or high-energy beta or alpha emitters (e.g. Lutetium-177 or Actinium-225) for radio-ligand therapy. Therefore, there is rising and increasing interest to explore the potential of PET/CT specimen imagers beyond ^{18}F-FDG, applying this high-resolution imaging in patients undergoing surgery for Pca or NET.

The aim of this pilot analysis was to assess the feasibility of a PET/CT specimen imager in a live-experience session in patients who received an intraoperative injection of ^{68}Ga-PSMA-11 and ^{68}Ga-DOTA-TOC.

2. Materials and Methods

2.1. Patient Population

This pilot analysis was performed as a secondary objective of two trials currently ongoing in our Institute in Pca (NCT05596851) and NET (NCT05448157) designed to evaluate the safety and the efficacy of a positron probe detector (DROP-IN β-probe) for live intra-operative radio-guided surgery. Three patients enrolled in these trials have been considered eligible for this supplemental analysis, two affected by Pca and one affected by NET of the ileum. In all cases, patients received a baseline whole-body PET/CT to assess the burden of the disease (^{68}Ga-PSMA-11 PET/CT and ^{68}Ga-DOTA-TOC PET/CT respectively). The scans were performed in the Division of Nuclear Medicine of our Institute (GE Discovery MIDR) according to international procedural guidelines, 4-6 weeks prior to surgery. All patients signed informed consent form prior to enrollment and studies have been approved by local ethical committee and scientific review board.

2.2. Specimen PET/CT imager

PET/CT images were obtained using the AURA10® Specimen PET/CT imager (Xeos Medical NV, Belgium). Subsequently, an optical, micro-CT and micro-PET images were acquired. The CT images were reconstructed using the Image Space Reconstruction Algorithm at 100μm voxel size. PET images were reconstructed using 20 iterations of the ordered subset expectation maximization algorithm at 400μm voxel size. The total duration between specimen insertion and visualization of the images on the device was 10 minutes.

 doi:10.20944/preprints202212.0444.v1

2.3. Description of the surgery procedure

The Pca patients received 1 MBq/kg of ^{68}Ga-PSMA-11 and the NET patient received 1.2 MBq/kg of ^{68}Ga-DOTA-TOC. PET radiopharmaceuticals administration was performed directly in the surgery theater at the beginning of the procedure. For Pca patients a robotic-assisted laparoscopic approach was adopted. Extended pelvic lymph node dissection (ePLND) was performed according to a standard template, including internal/external iliac nodes, obturatory nodes and common iliac ones. Radical prostatectomy (RP) was performed after ePLND, according to the study protocol (NCT05596851). For the ileum GEP-NET patient, open surgery was chosen as surgical approach, according to study protocol (NCT05448157).

In all cases, surgical specimens were collected in the operating theater and placed in dedicated containers by the pathologist, who oriented the specimens in the same position adopted for histopathological analysis. Specimen containers were placed in the PET/CT specimen imager and one scan was performed for each specimen. PET/CT acquisitions were performed 2,5 to 4,5 hours post-injection. Such delayed acquisition times can be made due to the high detection sensitivity of the Imager. Of some specimens, several acquisitions were performed, to explore the potential of administering less activity. High-resolution fused 3D images were obtained and reviewed in a multidisciplinary setting involving nuclear medicine physicians, surgeons, and pathologists. Pathologic assessment with immunohistochemistry (PSMA-staining and SSA immunoreactivity) was considered as standard of truth. Specimen images were subsequently compared with baseline PET/CT images and histopathological analysis.

3. Results

Patient n.1 was referred to PSMA-PET (Figure 1: A,E) for high-risk Pca (Gleason Score= 4+4; initial PSA= 10 ng/mL). PSMA-PET showed pathological and heterogeneous uptake diffusely comprising the left part of the prostate, without suspicion of extra-capsular extension. Additionally, five PSMA-positive pelvic lymph nodes were detected. According to E-PSMA reporting criteria (12) the patient was considered miT2N1M0. The day of surgery, 80 MBq of ^{68}Ga-PSMA-11 was administered intravenously. The prostate gland and pelvic lymph nodes were resected and all specimens were scanned in the PET/CT specimen imager. Scans were performed sequentially, once the specimens were positioned in the container and properly oriented by the pathologist, at 192 min (prostate) and 273 min (lymph nodes) post-injection. High-resolution PET/CT images (Figure 1: C,G) showed higher spatial resolution compared to conventional PET images, allowing a precise assessment of the surgical margins. Left basal margin's involvement was strongly suspected on the prostate gland image (Figure 1: C,D). All resected lymph nodes were scanned. Histopathology analysis was performed and compared with the specimen PET/CT images (Figure 1: D,H). For the prostate gland, the areas of PSMA-uptake in the micro-PET image corresponded to prostate cancer lesions on histopathological analysis. Extra-prostatic extension, as suspected from the micro-PET images, was also confirmed. Lymph nodes that showed PSMA uptake on micro-PET were confirmed to contain metastatic tumor cells on histopathological analysis. All positive lymph nodes detected in preoperative whole-body PET/CT were resected and imaged.

Preprints (www.preprints.org) | NOT PEER-REVIEWED | Posted: 23 December 2022 doi:10.20944/preprints202212.0444.v1

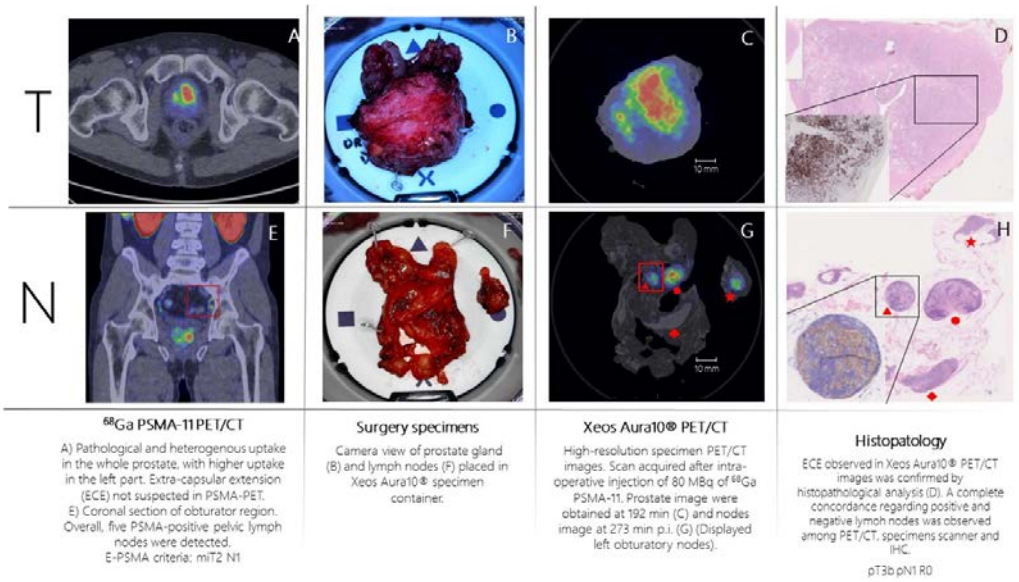

Figure 1. ^{68}Ga-PSMA-11 whole-body PET/CT images, high-resolution specimen PET/CT images and histopathological analysis obtained in patient-1 (prostate cancer).

Patient n.2 was referred to PSMA-PET (Figure 2: A,E,I) for high-risk Pca (Gleason Score= 4+5; initial PSA= 8 ng/mL). PSMA-PET showed pathological and heterogeneous uptake in the whole prostate, with suspicion of extra-capsular extension, two PSMA-positive pelvic lymph nodes and one PSMA-positive extra-pelvic lymph node. According to E-PSMA reporting criteria (12) the patient was considered miT3N1M1a. The day of surgery, 90 MBq of ^{68}Ga-PSMA-11 was administered intravenously. The prostate gland and lymph nodes were resected (Figure 2: B,F,J) and all specimens were scanned in the PET/CT specimen imager. Scans were performed sequentially, once the specimen was positioned in the container and properly oriented by the pathologist, at 206 min (prostate) and 265 min (lymph nodes) post-injection. Images (Figure 2: C,G,K) showed a high spatial resolution, and margin involvement was strongly suspected (Figure 2: C,D), in accordance with baseline PSMA-PET. PET/CT specimen images offered a high-resolution view of the distribution of PSMA inside the prostate lesion, highlighting high heterogeneity of PSMA expression in the prostate. As in the first case, areas of PSMA-uptake in the micro-PET image corresponded to prostate cancer lesions on histopathological analysis and a positive margin – as suspected from the microPET-CT images – was confirmed. Lymph nodes that showed PSMA uptake on micro-PET were confirmed to contain metastatic tumor cells on histopathological analysis.

Preprints (www.preprints.org) | NOT PEER-REVIEWED | Posted: 23 December 2022 doi:10.20944/preprints202212.0444.v1

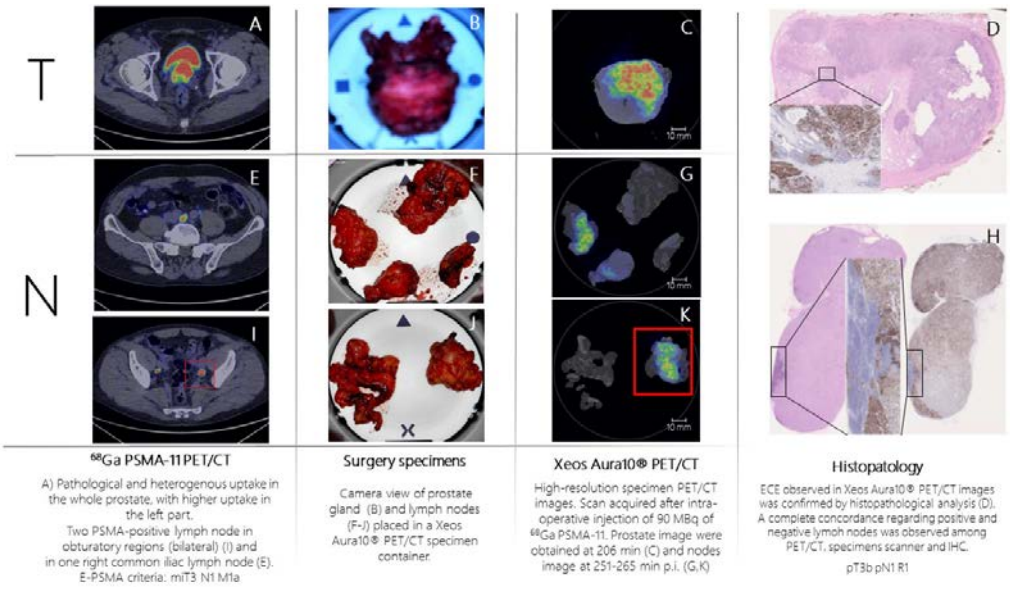

Figure 2. ^{68}Ga-PSMA-11 whole-body PET/CT images, high-resolution specimen PET/CT images and histopathological analysis obtained in patient-2 (prostate cancer).

Patient n.3 underwent ^{68}Ga-DOTA-TOC-PET (Figure 3: A) for recurrent ileum GEP-NET (G2; Ki-67= 5%). The PET scan showed the presence of a peri-pancreatic lymph node suspected of disease location. The day of surgery 70 MBq of ^{68}Ga-DOTA-TOC was administered intravenously. The PET-positive lymph node was resected and placed in the PET/CT specimen container. The specimen was scanned in the PET/CT specimen imager (Figure 3: B,C) at 150 minutes post-injection properly showing a high-resolution view of homogeneous ^{68}Ga-DOTA-TOC biodistribution within the lymph node. The specimen was analyzed for histopathology and 5mmune-histochemistry assessment with SSR 5mmune-reactivity (Figure3: D). A specipin was positioned in a region with high radiotracer uptake in the specimen as seen on the high-resolution PET/CT images. The positioning of this pin guided the pathologist to slice the specimen in the region of interest. This allowed an accurate comparison between the ^{68}Ga-DOTA-TOC uptake and the histopathological SSR immune-reactivity. All three methodologies (baseline PET/CT, specimen PET/CT and histopathology) were fully concordant, and the lymph node was considered as a true positive finding. Table 1 summarizes all semi-quantitative data about radiopharmaceuticals uptake both in whole-body PET/CT and high-resolution PET/CT specimen imaging.

Preprints (www.preprints.org) | NOT PEER-REVIEWED | Posted: 23 December 2022 doi:10.20944/preprints202212.0444.v1

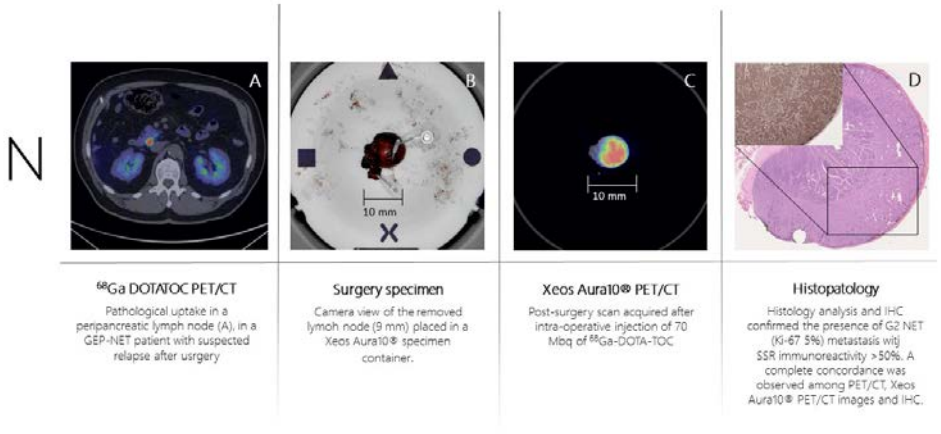

Figure 3. ^{68}Ga-DOTA-TOC whole-body PET/CT images, high-resolution specimen PET/CT images and histopathological analysis obtained in patient-3 (GEP-NET).

Table 1. Semi-quantitative data measured both in pre-operative whole-body PET/CT and high-resolution specimen PET/CT images.

	PET/CT SUVmax	Specimen Imager SUVmax
Pt-1 Prostate	26.5	89.2
Pt-1 Left Obturatory Nodes	11.4	51.5
Pt-2 Prostate	36.2	57.4
Pt-2 Right Common Iliac Node	11.8	23.2
Pt-2 Left Obturatory Nodes	25.9	36.4
Pt-3 Peri-pancreatic Node	52.1	86.6

SUVmax: Maximum Standardized Uptake Value

Finally, in all procedures the radiation exposure of the operating theater staff located near the surgical table was measured using an Electronic Personal Dosimeters (Thermo Scientific™ EPD Mk2™) and the absorbed dose was below 40 μSv (range 26 – 40 μSv) for each procedure.

4. Discussion

In this pilot analysis, first we assessed the feasibility of integrating this new generation imaging approach in a live-surgery session. The collection and the scan of the specimens did not significantly interfere with any procedure, and the overall length of the surgery was not affected using the PET/CT specimen imager. Second, the radiation exposure generally measured for radio-guided surgery using gamma emitting isotopes (e.g., ^{99m}Tc or ^{18}F) is low and this technique is extensively used in clinical practice. With ^{99m}Tc radiation doses per procedure to the surgeon's chest is comprised between 0.2–0.8 μSv per MBq of activity present at time of surgery, while for ^{18}F radiation exposures to the surgeon's chest is comprised between 10 to 217 μSv for procedures [13]. The radiation exposure for the operating theater staff measured in our pilot analysis was low as well (less than 40 μSv range 26 – 40 μSv), confirming the feasibility of injecting positron emitting isotopes (e.g., ^{68}Ga or ^{18}F) directly in the surgery theater. Finally, the specimen PET images were reliable, and in full concordance with the information derived by the histopathological analysis. Moreover, they had a higher spatial resolution compared to conventional PET images. The extraction of semiquantitative parameters (e.g., SUVmax or metabolic tumor volume) was also feasible.

 doi:10.20944/preprints202212.0444.v1

At present, the implementation in clinical practice of this device has not been broadly explored. However, the development of PET/CT specimen imagers has a promising perspective and embraces the integration of new generation imaging with the most updated surgery techniques. This new approach might improve surgeon's confidence in ensuring complete removal of the primary tumor. Moreover, the precise correspondence of receptor-target radiopharmaceuticals uptake and immuno-histochemistry staining confirmed the precision of this imaging procedure to evaluate intra-lesion heterogeneity. Thus, the high spatial resolution of the PET specimen imager offers a deeper understanding of the bio-distribution pattern of the radiotracers inside cancer lesions. In this scenario, the use of a specimen imager might be an adjunct tool for the pathologist to better optimize resources and for a "live" assessment of specific tumor biomarkers directly during surgery.

Another potential advantage might be related to the high negative predictive value (NPV) of this imaging procedure. In patient 1 and 2, histopathology confirmed the lymph node showing high PSMA expression as true positive findings. However, also PSMA negative nodes were included in the specimen container. The histopathological analysis confirmed the lack of malignant cells in these lymph nodes, thus resulting as true negative findings. The future challenge will be understanding if the PET/CT specimen imager might detect micro-metastasis. Furthermore, in patient 1 extra-capsular extension was not suspected in baseline PSMA PET/CT. However, extra-capsular extension was observed with the specimen imager (and subsequently confirmed by histology), thus hinting at a potential superior sensitivity compared to the whole-body PET images used in clinical practice.

In clinical practice, new generation molecular imaging has already proven its crucial role in the decision-making process of several malignancies, including PCa and NET, and the transition from pre-clinical imaging to clinical practice has been quick and clinically significant. However, new radiopharmaceuticals are emerging beyond PSMA and SSR based PET, like inhibitors of the fibroblast activating protein (FAPi PET) or ligand of the chemokine receptor 4 CXCR4 (Pentixafor PET). All these new radiopharmaceuticals will increase the number of pathways that can be explored with in vivo molecular imaging, and it will increase the understanding of tumor heterogeneity both in primary tumor and in metastatic locations. In this scenario, intra-operative PET/CT specimen imaging offers a link between molecular biology, histopathology assessment, molecular imaging and radio-guided surgery.

5. Conclusion

The use of the PET/CT specimen imager in a live-experience session was feasible and its application has been easily adapted to surgery daily-practice. The image acquisition of specimens obtained by patients who received intra-surgery injection of ^{68}Ga-PSMA-11 and ^{68}Ga-DOTA-TOC was feasible and reliable, and the imaging findings matched perfectly with histopathological analysis. The high sensitivity, together with the evaluation of intra-lesion tumor heterogeneity, were the most relevant results derived from this pilot analysis. Even if far from definitive evidence, this pilot analysis showed promising results that need to be confirmed by further prospective analysis in larger cohorts of oncological patients.

References

1. Kapoor V, McCook BM, Torok FS. An introduction to PET-CT imaging. Radiographics. 2004 Mar-Apr;24(2):523-43. doi: 10.1148/rg.242025724. PMID: 15026598.
2. Slart RHJA, Tsoumpas C, Glaudemans AWJM, Noordzij W, Willemsen ATM, Borra RJH, Dierckx RAJO, Lammertsma AA. Long axial field of view PET scanners: a road map to implementation and new possibilities. Eur J Nucl Med Mol Imaging. 2021 Dec;48(13):4236-4245. doi: 10.1007/s00259-021-05461-6. Epub 2021 Jun 16. PMID: 34136956; PMCID: PMC8566640.
3. Göker, M., Vergauwen, G., Van de Velde, C., Van de Vijver, K., Van de Sande, L., Keereman, V., 2021. Peri-operative 18F-FDG-PET-CT specimen imaging for margin assessment in breast malignancies: a proof-of-concept study. Abstract and Poster presentation – ESSO.

4. Debacker, J.M., Schelfhout, V., Brochez, L., Creytens, D., D'Asseler, Y., Deron, P., Keereman, V., Van de Vijver, K., Vanhove, C., Huvenne, W., 2021. High-Resolution 18F-FDG PET/CT for Assessing Three-Dimensional Intraoperative Margins Status in Malignancies of the Head and Neck, a Proof-of-Concept. J Clin Med 10, 3737.
5. Maris, L., De Man, K., Gryspeerdt, F., Hoorens, A., Keereman, V., Kiekens, A., Van den Broeck, B., Van de Sande, L., Vanhove, C., Berrevoet, F., 2022. 18F-FDG-PET-CT specimen imaging for perioperative visualization of pancreatic adenocarcinoma: a proof-of-concept study. Abstract and Poster presentation – ESSO.
6. Hofman MS, Lawrentschuk N, Francis RJ, et al. Prostate-specific membrane antigen PET-CT in 404 patients with high-risk prostate cancer before curative-intent surgery or radiotherapy (proPSMA): a 405 prospective, randomised, multicentre study. Lancet. 2020;395(10231):1208-1216. 406 doi:10.1016/S0140-6736(20)30314-7 407;
7. Emmett L, Buteau J, Papa N, Moon D, Thompson J, Roberts MJ, et al. The Additive Diagnostic 408 Value of Prostate-specific Membrane Antigen Positron Emission Tomography Computed 409 Tomography to Multiparametric Magnetic Resonance Imaging Triage in the Diagnosis of Prostate 410 Cancer (PRIMARY): A Prospective Multicentre Study. European Urology. 2021;80(6):682-9. doi: 411 10.1016/j.eururo.2021.08.002;
8. Calais J, Ceci F, Eiber M, Hope TA, Hofman MS, Rischpler C, Bach-Gansmo T, Nanni C, Savir-Baruch B, Elashoff D, Grogan T, Dahlbom M, Slavik R, Gartmann J, Nguyen K, Lok V, Jadvar H, Kishan AU, Rettig MB, Reiter RE, Fendler WP, Czernin J. ^{18}F-fluciclovine PET-CT and ^{68}Ga-PSMA-11 PET-CT in patients with early biochemical recurrence after prostatectomy: a prospective, single-centre, single-arm, comparative imaging trial. Lancet Oncol. 2019 Sep;20(9):1286-1294. doi: 10.1016/S1470-2045(19)30415-2. Epub 2019 Jul 30. Erratum in: Lancet Oncol. 2019 Nov;20(11):e613. Erratum in: Lancet Oncol. 2020 Jun;21(6):e304. PMID: 31375469; PMCID: PMC7469487.
9. Hope TA, Eiber M, Armstrong WR, Juarez R, Murthy V, Lawhn-Heath C, Behr SC, Zhang L, Barbato F, Ceci F, Farolfi A, Schwarzenböck SM, Unterrainer M, Zacho HD, Nguyen HG, Cooperberg MR, Carroll PR, Reiter RE, Holden S, Herrmann K, Zhu S, Fendler WP, Czernin J, Calais J. Diagnostic Accuracy of 68Ga-PSMA-11 PET for Pelvic Nodal Metastasis Detection Prior to Radical Prostatectomy and Pelvic Lymph Node Dissection: A Multicenter Prospective Phase 3 Imaging Trial. JAMA Oncol. 2021 Nov 1;7(11):1635-1642. doi: 10.1001/jamaoncol.2021.3771. PMID: 34529005; PMCID: PMC8446902.
10. Fendler WP, Calais J, Eiber M, Flavell RR, Mishoe A, Feng FY, Nguyen HG, Reiter RE, Rettig MB, Okamoto S, Emmett L, Zacho HD, Ilhan H, Wetter A, Rischpler C, Schoder H, Burger IA, Gartmann J, Smith R, Small EJ, Slavik R, Carroll PR, Herrmann K, Czernin J, Hope TA. Assessment of 68Ga-PSMA-11 PET Accuracy in Localizing Recurrent Prostate Cancer: A Prospective Single-Arm Clinical Trial. JAMA Oncol. 2019 Jun 1;5(6):856-863. doi: 10.1001/jamaoncol.2019.0096. PMID: 30920593; PMCID: PMC6567829.
11. Bozkurt MF, Virgolini I, Balogova S, Beheshti M, Rubello D, Decristoforo C, Ambrosini V, Kjaer A, Delgado-Bolton R, Kunikowska J, Oyen WJG, Chiti A, Giammarile F, Sundin A, Fanti S. Guideline for PET/CT imaging of neuroendocrine neoplasms with 68Ga-DOTA-conjugated somatostatin receptor targeting peptides and 18F-DOPA. Eur J Nucl Med Mol Imaging. 2017 Aug;44(9):1588-1601. doi: 10.1007/s00259-017-3728-y. Epub 2017 May 25. Erratum in: Eur J Nucl Med Mol Imaging. 2017 Aug 30;: PMID: 28547177.
12. Ceci F, Oprea-Lager DE, Emmett L, Adam JA, Bomanji J, Czernin J, Eiber M, Haberkorn U, Hofman MS, Hope TA, Kumar R, Rowe SP, Schwarzenboeck SM, Fanti S, Herrmann K. E-PSMA: the EANM standardized reporting guidelines v1.0 for PSMA-PET. Eur J Nucl Med Mol Imaging. 2021 May;48(5):1626-1638. doi: 10.1007/s00259-021-05245-y. Epub 2021 Feb 19. PMID: 33604691; PMCID: PMC8113168.
13. With Tc99m, radiation doses per procedure to the surgeon's torso vary in the ranges 0.2–0.8 μSv per MBq of activity present at time of surgery; while for F-18 radiation exposures to the surgeon's torso ranges between 10 to 217 for procedures [X]